Structural Monitoring and Maintenance, *Vol. 7, No. 1 (2020) 27-42*
DOI: https://doi.org/10.12989/smm.2020.7.1.027

A numerical method for dynamic characteristics of nonlocal porous metal-ceramic plates under periodic dynamic loads

Mohammed Abdulraoof Abdulrazzaq, Zeyad D. Kadhim,
Nadhim M. Faleh* and Nader M. Moustafa

Al-Mustansiriah University, Engineering Collage P.O. Box 46049, Bab-Muadum, Baghdad 10001, Iraq

(Received August 13, 2019, Revised November 10, 2019, Accepted November 15, 2019)

Abstract. Dynamic stability of graded nonlocal nano-dimension plates on elastic substrate due to in-plane periodic loads has been researched via a novel 3- unknown plate theory based on exact position of neutral surface. Proposed theory confirms the shear deformation effects and contains lower field components in comparison to first order and refined 4- unknown plate theories. A modified power-law function has been utilized in order to express the porosity-dependent material coefficients. The equations of nanoplate have been represented in the context of Mathieu–Hill equations and Chebyshev-Ritz-Bolotin's approach has been performed to derive the stability boundaries. Detailed impacts of static/dynamic loading parameters, nonlocal constant, foundation parameters, material index and porosities on instability boundaries of graded nanoscale plates are researched.

Keywords: dynamic instability; 3- unknown plate theory; FGM nanoplate; nonlocal theory, porosities

1. Introduction

Functionally graded materials (FGMs) contains two constituents which are usually ceramic and metal in a combined form. In fact, the material formation is graded between ceramic and metal and porosities will produce due to imperfect combination of the two phases. The material characteristics of FGMs may be described based on the portion of these two phases and also porosity amount (Atmane *et al*. 2015a, b). However, providing many outstanding properties, FG materials will be used in different engineering sections including mechanical and civil engineering (Ahmed *et al.* 2018, Faleh *et al*. 2018, Thai *et al*. 2014, She *et al*. 2018a, b, 2019a, b, Shafiei and She 2018).

Recently, engineering structures have been used in the production of nano-size devices and objects. Some of these structures have beam or plate shapes having nano dimensions (Zenkour 2016, She *et al*. 2017, Zenkour 2018, 2019). The most important issue about these structures is understanding their mechanical characteristics such as dynamic behaviors. However, such an investigation needs refined continuum mechanics due to nano dimension effects since classical mechanics is impotent to express such effects. To this end, nonlocal elasticity theory (Eringen 1983) is proposed to make the researchers able to analysis mechanical characteristics of nano-size structures. The theory proposed a modified stress-strain relation based on nonlocal parameter in

*Corresponding author, Professor, E-mail: dr.nadhim@uomustansiriyah.edu.iq

Copyright © 2020 Techno-Press, Ltd.
http://www.techno-press.org/?journal=smm&subpage=7 ISSN: 2288-6605 (Print), 2288-6613 (Online)

order to formulate nano-structures. This relation is used by many researches to provide suitable formulations for nano-structures (Zemri *et al*. 2015, Larbi Chaht *et al*. 2015, Cherif *et al.* 2018, Khetir *et al*. 2017, Karami *et al*. 2017,2018, Bouafia *et al.* 2017, Bouadi *et al*. 2018, Mouffoki *et al*. 2017, Bellifa *et al*. 2017, Mokhtar *et al*. 2018, Yazid *et al*. 2018, Karami *et al*. 2018a, b, Shahverdi and Barati 2017, Malikan *et al.* 2018). The theory is also applicable for nano-structures made of FGMs. Natarajan et al. (2012) explored finite element based vibrational response of graded nanosize plates with simply-supported and clamped edges. Belkorissat *et al*. (2015) examined vibrational characteristics of graded nanosize plates by introducing a size-dependent four-unknown plate theory. They showed that the classical plate model cannot consider the shear deformation mechanism and proposed a more accurate theory containing a shear stress function. So, higher order theories such as third-order (Reddy 1990), 4-unknown and 3-unknown theories are more applicable for thick plates (Tai *et al*. 2013, Zenkour 2009, Mehala *et al.* 2018, Sadoun *et al*. 2018, Mahmoudi *et al.* 2018, Houari *et al.* 2016, Belabed *et al*. 2018). Also, Hosseini and Jamalpoor (2015) presented an analytical investigation of thermo-mechanical vibration behavior of bilayer FG nanoplates in elastic medium. Mechab *et al.* (2016) presented the size-dependent and porosity-dependent analysis of FG nanoplates lying on an elastic substrate. All of above researches on FG nano-size plates studied their static stability or free vibration behavior. Thus, dynamic instability of 3-unkown FG nano-size plates under in-plane periodic loads is not studied yet.

In this research, dynamic instability properties of a FG nanoplate exposed to in-plane periodic loads have been researched via a novel 3- unknown plate theory based on exact position of neutral surface. Proposed theory confirms the shear deformations impacts and contains lower field components in comparison to first order and refined 4- unknown plate theories. A modified power-law function has been utilized in order to express the porosity-dependent material coefficients. The equations of nanoplate have been represented with the form of Mathieu–Hill equations and Chebyshev-Ritz-Bolotin's method has been performed to derive the stability boundaries. Detailed impacts of static/dynamic loading parameters, nonlocal constant, foundation parameters, material index and porosities on instability boundaries of graded nanoscale plates are studied.

2. Governing equations

2.1 Modeling of FG nanoplates

Assume a rectangular FG nanoplate with thickness h as illustrated in Fig. 1. A FG material may be specified by changing of the volume fractions. Based upon the modified power-law model, Young' modulus E and density ρ are described as (Yahia *et al*. 2015)

$$E(z) = (E_c - E_m)\left(\frac{z}{h} + \frac{1}{2}\right)^p + E_m - \frac{\xi}{2}(E_c + E_m) \tag{1a}$$

$$\rho(z) = (\rho_c - \rho_m)\left(\frac{z}{h} + \frac{1}{2}\right)^p + \rho_m - \frac{\xi}{2}(\rho_c + \rho_m) \tag{1b}$$

in which z is the distance from the mid-surface of the plate. Also, c and m are corresponding to material properties related to ceramic and metallic constituents, respectively and p denotes inhomogeneity or power-law index. Moreover, ξ defines the porosity volume fraction.

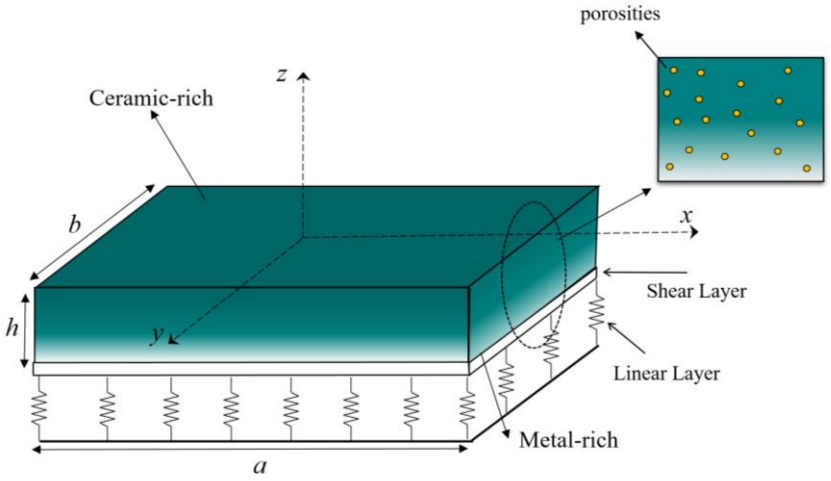

Fig. 1 A FGM nanoplate having porosities rested on elastic substrate

Based on nonlocal elasticity theory, the nonlocality of stress field can be incorporated into the stress-strain relationship as

$$(1-(e_0a)\nabla^2)\sigma_{ij}=\varepsilon_{kl} \tag{2}$$

in which ∇^2 is the Laplacian operator and $e_0 a$ is the scale parameter which considers the small size effect. Also, σ_{ij} and ε_{kl} respectively denote the stress and strain field components.

Finally, the nonlocal constitutive relations based on refined FG plate model can be expressed by

$$(1-(e_0a)\nabla^2)\begin{Bmatrix}\sigma_{xx}\\ \sigma_{yy}\\ \sigma_{xy}\\ \sigma_{yz}\\ \sigma_{xz}\end{Bmatrix}=\begin{pmatrix}Q_{11} & Q_{12} & 0 & 0 & 0\\ Q_{12} & Q_{22} & 0 & 0 & 0\\ 0 & 0 & Q_{66} & 0 & 0\\ 0 & 0 & 0 & Q_{44} & 0\\ 0 & 0 & 0 & 0 & Q_{55}\end{pmatrix}\begin{Bmatrix}\varepsilon_{xx}\\ \varepsilon_{yy}\\ \gamma_{xy}\\ \gamma_{yz}\\ \gamma_{xz}\end{Bmatrix} \tag{3}$$

where

$$Q_{11}=Q_{22}=\frac{E(z)}{1-\upsilon^2},\ Q_{12}=\upsilon Q_{11},\ Q_{44}=Q_{55}=Q_{66}=\frac{E(z)}{2(1+\upsilon)}$$

2.2 Formulation based on 3-unknown theory

Modeling of the nanoplate is performed employing a 3-unknown plate theory which has fewer field unknowns compared with the refined 4-unknown and also first order plate theory (Zidi *et al*. 2017, Kaci *et al*. 2018, Hachemi *et al*. 2017). The three dimensional displacement field (u_x, u_y, u_z) of the 3-unknown plate model can be expressed by

$$u_x(x,y,z,t) = u(x,y,t) - z\frac{\partial w}{\partial x} - \Gamma(z)\frac{\partial^3 w}{\partial x^3} \tag{4}$$

$$u_y(x,y,z,t) = v(x,y,t) - z\frac{\partial w}{\partial y} - \Gamma(z)\frac{\partial^3 w}{\partial y^3} \tag{5}$$

$$u_z(x,y,z,t) = w(x,y,t) \tag{6}$$

Here, u and v are in-plane displacements and w denotes the transverse displacement; $\Gamma(z)$ is shear deformation function. For more accurate modeling of FGM structures, it is crucial to consider the exact positions of neutral surface. Generally, there is coupling between in-plane and out-of-plane displacements of FGM plates, as it can be seen in Eqs. (4) and (5). By considering the exact position of neutral surface, it is possible to eliminate this coupling. So, the displacement field of 3-unknown plate model can be reduced to the following form:

$$u_x(x,y,z,t) = -(z-z^*)\frac{\partial w}{\partial x} - (\Gamma(z)-z^{**})\frac{\partial^3 w}{\partial x^3} \tag{7}$$

$$u_y(x,y,z,t) = -(z-z^*)\frac{\partial w}{\partial y} - (\Gamma(z)-z^{**})\frac{\partial^3 w}{\partial y^3} \tag{8}$$

$$u_z(x,y,z,t) = w(x,y,t) \tag{9}$$

It is evident that the displacement field is reduced to a single-unknown model and the location parameters of neutral surface are (Han *et al.* 2015)

$$z^* = \frac{\int_{-h/2}^{h/2} E(z)\, z dz}{\int_{-h/2}^{h/2} E(z)\, dz}, \quad z^{**} = \frac{\int_{-h/2}^{h/2} E(z)\Gamma(z) dz}{\int_{-h/2}^{h/2} E(z)\, dz} \tag{10}$$

In the present paper, the shear deformation function has been selected as

$$\Gamma(z) = \cosh\left(\frac{\pi}{2}\right)\frac{h^3}{2\pi^2}\sin\left(\frac{\pi z}{h}\right) \tag{11}$$

Finally, the strains based on the three-unknown plate model are obtained as

$$\begin{Bmatrix}\varepsilon_x\\ \varepsilon_y\\ \gamma_{xy}\end{Bmatrix} = \begin{Bmatrix}\varepsilon_x^0\\ \varepsilon_y^0\\ \gamma_{xy}^0\end{Bmatrix} + z\begin{Bmatrix}\kappa_x\\ \kappa_y\\ \kappa_{xy}\end{Bmatrix} + \Gamma(z)\begin{Bmatrix}\eta_x\\ \eta_y\\ \eta_{xy}\end{Bmatrix}, \quad \begin{Bmatrix}\gamma_{yz}\\ \gamma_{xz}\end{Bmatrix} = g(z)\begin{Bmatrix}\gamma_{yz}^0\\ \gamma_{xz}^0\end{Bmatrix} \tag{12}$$

where $g(z) = \Gamma'(z)$ and

$$\begin{Bmatrix}\varepsilon_x^0\\ \varepsilon_y^0\\ \gamma_{xy}^0\end{Bmatrix}=\begin{Bmatrix}\frac{\partial u}{\partial x}\\ \frac{\partial v}{\partial y}\\ \frac{\partial u}{\partial y}+\frac{\partial v}{\partial x}\end{Bmatrix},\begin{Bmatrix}\kappa_x\\ \kappa_y\\ \kappa_{xy}\end{Bmatrix}=\begin{Bmatrix}-\frac{\partial^2 w}{\partial x^2}\\ -\frac{\partial^2 w}{\partial y^2}\\ -2\frac{\partial^2 w}{\partial x\partial y}\end{Bmatrix},\begin{Bmatrix}\eta_x\\ \eta_y\\ \eta_{xy}\end{Bmatrix}=\begin{Bmatrix}-\frac{\partial^4 w}{\partial x^2}\\ -\frac{\partial^4 w}{\partial y^4}\\ -\frac{\partial^2(\nabla^2 w)}{\partial x\partial y}\end{Bmatrix},\begin{Bmatrix}\gamma_{yz}^0\\ \gamma_{xz}^0\end{Bmatrix}=\begin{Bmatrix}\frac{\partial^3 w}{\partial y^3}\\ \frac{\partial^3 w}{\partial x^3}\end{Bmatrix} \quad (13)$$

The strain energy may be defined by

$$U=0.5\int_V \sigma_{ij}\,\varepsilon_{ij}\,dV=\int_V(\sigma_x\,\varepsilon_{xx}+\sigma_y\,\varepsilon_{yy}+\sigma_{xz}\,\gamma_{xz}+\sigma_{xy}\,\gamma_{xy}+\sigma_{yz}\gamma_{yz})\,dV \quad (14)$$

Inserting Eqs. (12) and (13) into Eq.(14) yields

$$\begin{aligned}U=0.5\int_{-0.5a}^{0.5a}\int_{-0.5b}^{0.5b}[&A_{11}\frac{\partial u}{\partial x}\frac{\partial u}{\partial x}-2B_{11}\frac{\partial u}{\partial x}\frac{\partial^2 w}{\partial x^2}-2B_{11}^s\frac{\partial u}{\partial x}\frac{\partial^4 w}{\partial x^4}+2D_{11}^s\frac{\partial^2 w}{\partial x^2}\frac{\partial^4 w}{\partial x^4}\\
&+D_{11}\frac{\partial^2 w}{\partial x^2}\frac{\partial^2 w}{\partial x^2}+H_{11}^s\frac{\partial^4 w}{\partial x^4}\frac{\partial^4 w}{\partial x^4}+2A_{12}\frac{\partial u}{\partial x}\frac{\partial v}{\partial y}-2B_{12}\frac{\partial u}{\partial x}\frac{\partial^2 w}{\partial y^2}-2B_{12}^s\frac{\partial u}{\partial x}\frac{\partial^4 w}{\partial y^4}\\
&+2D_{12}^s\frac{\partial^2 w}{\partial x^2}\frac{\partial^4 w}{\partial y^4}+2D_{12}^s\frac{\partial^4 w}{\partial x^4}\frac{\partial^2 w}{\partial y^2}+2D_{12}\frac{\partial^2 w}{\partial x^2}\frac{\partial^2 w}{\partial y^2}+2H_{12}^s\frac{\partial^4 w}{\partial x^4}\frac{\partial^4 w}{\partial y^4}\\
&-2B_{12}\frac{\partial v}{\partial x}y\frac{\partial^2 w}{\partial x^2}-2B_{12}^s\frac{\partial v}{\partial y}\frac{\partial^4 w}{\partial x^4}+A_{11}\frac{\partial v}{\partial y}\frac{\partial v}{\partial y}-2B_{11}\frac{\partial v}{\partial y}\frac{\partial^2 w}{\partial y^2}-2B_{11}^s\frac{\partial v}{\partial y}\frac{\partial^4 w}{\partial y^4}\\
&+2D_{11}^s\frac{\partial^2 w}{\partial y^2}\frac{\partial^4 w}{\partial y^4}+D_{11}\frac{\partial^2 w}{\partial y^2}\frac{\partial^2 w}{\partial y^2}+H_{11}^s\frac{\partial^4 w}{\partial y^4}\frac{\partial^4 w}{\partial y^4}\\
&+A_{66}(\frac{\partial u}{\partial y}\frac{\partial u}{\partial y}+2\frac{\partial v}{\partial x}\frac{\partial u}{\partial y}+\frac{\partial v}{\partial x}\frac{\partial v}{\partial x})-4B_{66}(\frac{\partial u}{\partial y}+\frac{\partial v}{\partial x})\frac{\partial^2 w}{\partial x\partial y}\\
&-4B_{66}^s(\frac{\partial u}{\partial y}+\frac{\partial v}{\partial x})\frac{\partial^2(\nabla^2 w)}{\partial x\partial y}+4D_{66}\frac{\partial^2 w}{\partial x\partial y}\frac{\partial^2 w}{\partial x\partial y}+4D_{66}^s\frac{\partial^2 w}{\partial x\partial y}\frac{\partial^2(\nabla^2 w)}{\partial x\partial y}\\
&+2H_{66}^s\frac{\partial^2(\nabla^2 w)}{\partial x\partial y}\frac{\partial^2(\nabla^2 w)}{\partial x\partial y}+A_{55}^s\frac{\partial^3 w}{\partial y^3}\frac{\partial^3 w}{\partial y^3}+A_{44}^s\frac{\partial^3 w}{\partial x^3}\frac{\partial^3 w}{\partial x^3}]dxdy\end{aligned} \quad (15)$$

The work of non-conservative forces is expressed by

$$\begin{aligned}V=0.5\int_{-0.5a}^{0.5a}\int_{-0.5b}^{0.5b}(&N_x^0\frac{\partial w}{\partial x}\frac{\partial w}{\partial x}+\mu N_x^0\frac{\partial^2 w}{\partial x^2}\frac{\partial^2 w}{\partial x^2}+N_y^0\frac{\partial w}{\partial y}\frac{\partial w}{\partial y}+\mu N_y^0\frac{\partial^2 w}{\partial y^2}\frac{\partial^2 w}{\partial y^2}\\
&-k_w w-\mu k_w\frac{\partial w}{\partial x}\frac{\partial w}{\partial x}+k_p\frac{\partial w}{\partial x}\frac{\partial w}{\partial x}+\mu\frac{\partial^2 w}{\partial x^2}\frac{\partial^2 w}{\partial x^2})dydx\end{aligned} \quad (16)$$

where N_x^0, N_y^0 are interior applied forces and k_w, k_p define elastic substrate constants. Next, the kinetic energy is obtained as

$$K = 0.5\int_{-0.5a}^{0.5a}\int_{-0.5b}^{0.5b}[I_0(\frac{\partial w}{\partial t}\frac{\partial w}{\partial t}+\frac{\partial v}{\partial t}\frac{\partial v}{\partial t}+\frac{\partial u}{\partial t}\frac{\partial u}{\partial t})+\mu I_0(\frac{\partial^2 w}{\partial x\partial t}\frac{\partial^2 w}{\partial x\partial t}+\frac{\partial^2 v}{\partial x\partial t}\frac{\partial^2 v}{\partial x\partial t}+\frac{\partial^2 u}{\partial x\partial t}\frac{\partial^2 u}{\partial x\partial t}$$
$$+\frac{\partial^2 w}{\partial y\partial t}\frac{\partial^2 w}{\partial y\partial t}+\frac{\partial^2 u}{\partial y\partial t}\frac{\partial^2 u}{\partial y\partial t}+\frac{\partial^2 v}{\partial y\partial t}\frac{\partial^2 v}{\partial y\partial t})-I_1(\frac{\partial u}{\partial t}\frac{\partial^2 w}{\partial x\partial t}+\frac{\partial v}{\partial t}\frac{\partial^2 w}{\partial y\partial t})-\mu I_1(\frac{\partial^2 u}{\partial y\partial t}\frac{\partial^3 w}{\partial x\partial y\partial t}+\frac{\partial^2 u}{\partial x\partial t}\frac{\partial^3 w}{\partial x^2\partial t}$$
$$+\frac{\partial^2 v}{\partial y\partial t}\frac{\partial^3 w}{\partial y^2\partial t}+\frac{\partial^2 v}{\partial x\partial t}\frac{\partial^3 w}{\partial x\partial y\partial t})-J_1(+\frac{\partial v}{\partial t}\frac{\partial^4 w}{\partial y^3\partial t}\frac{\partial u}{\partial t}\frac{\partial^4 w}{\partial x^3\partial t})-\mu J_1(\frac{\partial^2 u}{\partial y\partial t}\frac{\partial^5 w}{\partial x^3\partial y\partial t}+\frac{\partial^2 u}{\partial x\partial t}\frac{\partial^5 w}{\partial x^4\partial t}$$
$$+\frac{\partial^2 v}{\partial y\partial t}\frac{\partial^5 w}{\partial y^4\partial t}+\frac{\partial^2 v}{\partial x\partial t}\frac{\partial^5 w}{\partial x\partial y^3\partial t})+I_2(+\frac{\partial^2 w}{\partial y\partial t}\frac{\partial^2 w}{\partial y\partial t}+\frac{\partial^2 w}{\partial x\partial t}\frac{\partial^2 w}{\partial x\partial t})+\mu I_2(\frac{\partial^3 w}{\partial x^2\partial t}\frac{\partial^3 w}{\partial x^2\partial t}$$
$$+2\frac{\partial^3 w}{\partial x\partial y\partial t}\frac{\partial^3 w}{\partial x\partial y\partial t}+\frac{\partial^3 w}{\partial y^2\partial t}\frac{\partial^3 w}{\partial y^2\partial t})+K_2(\frac{\partial^4 w}{\partial x^3\partial t}\frac{\partial^4 w}{\partial x^3\partial t}+\frac{\partial^4 w}{\partial y^3\partial t}\frac{\partial^4 w}{\partial y^3\partial t})+\mu K_2(\frac{\partial^5 w}{\partial x^4\partial t}\frac{\partial^5 w}{\partial x^4\partial t}$$
$$+\frac{\partial^5 w}{\partial x^3\partial y\partial t}\frac{\partial^5 w}{\partial x^3\partial y\partial t}+\frac{\partial^5 w}{\partial x\partial y^3\partial t}\frac{\partial^5 w}{\partial x\partial y^3\partial t}+\frac{\partial^5 w}{\partial y^4\partial t}\frac{\partial^5 w}{\partial y^4\partial t})+J_2(\frac{\partial^2 w}{\partial x\partial t}\frac{\partial^4 w}{\partial x^3\partial t}+\frac{\partial^2 w}{\partial y\partial t}\frac{\partial^4 w}{\partial y^3\partial t})$$
$$+\mu J_2(\frac{\partial^3 w}{\partial x^2\partial t}\frac{\partial^5 w}{\partial x^4\partial t}+\frac{\partial^3 w}{\partial x\partial y\partial t}\frac{\partial^5 w}{\partial x^3\partial y\partial t}+\frac{\partial^3 w}{\partial x\partial y\partial t}\frac{\partial^5 w}{\partial x\partial y^3\partial t}+\frac{\partial^3 w}{\partial y^2\partial t}\frac{\partial^5 w}{\partial y^4\partial t})]dydx \tag{17}$$

Where

$$(I_0, I_1, J_1, I_2, J_2, K_2) = \int_{-h/2}^{h/2}(1, z, \Gamma, z^2, z\Gamma, \Gamma^2)\rho(z)dz \tag{18}$$

and

$$\begin{Bmatrix} A_{11}, B_{11}, B_{11}^s, D_{11}, D_{11}^s, H_{11}^s \\ A_{12}, B_{12}, B_{12}^s, D_{12}, D_{12}^s, H_{12}^s \\ A_{66}, B_{66}, B_{66}^s, D_{66}, D_{66}^s, H_{66}^s \end{Bmatrix} = \int_{-h/2}^{h/2} Q_{11}(1, z, \Gamma, z^2, z\Gamma, \Gamma^2)\begin{Bmatrix} 1 \\ \upsilon \\ \frac{1-\upsilon}{2} \end{Bmatrix}dz \tag{19}$$

$$A_{44}^s = A_{55}^s = \int_{-h/2}^{h/2} g^2 \frac{E(z)}{2(1+\upsilon)}dz \tag{20}$$

As mentioned, bending-extension coupling eliminates by incorporation of neutral surface position. Eqs. (15) and (17) can be reduced in term of w by discarding u and v as

$$U = 0.5\int_{-0.5a}^{0.5a}\int_{-0.5b}^{0.5b}[+2\tilde{D}_{11}^s\frac{\partial^2 w}{\partial x^2}\frac{\partial^4 w}{\partial x^4}+\tilde{D}_{11}\frac{\partial^2 w}{\partial x^2}\frac{\partial^2 w}{\partial x^2}+\tilde{H}_{11}^s\frac{\partial^4 w}{\partial x^4}\frac{\partial^4 w}{\partial x^4}$$
$$+2\tilde{D}_{12}^s\frac{\partial^2 w}{\partial x^2}\frac{\partial^4 w}{\partial y^4}+2\tilde{D}_{12}^s\frac{\partial^4 w}{\partial x^4}\frac{\partial^2 w}{\partial y^2}+2\tilde{D}_{12}\frac{\partial^2 w}{\partial x^2}\frac{\partial^2 w}{\partial y^2}+2\tilde{H}_{12}^s\frac{\partial^4 w}{\partial x^4}\frac{\partial^4 w}{\partial y^4}$$
$$+2\tilde{D}_{11}^s\frac{\partial^2 w}{\partial y^2}\frac{\partial^4 w}{\partial y^4}+\tilde{D}_{11}\frac{\partial^2 w}{\partial y^2}\frac{\partial^2 w}{\partial y^2}+\tilde{H}_{11}^s\frac{\partial^4 w}{\partial y^4}\frac{\partial^4 w}{\partial y^4}$$
$$+4\tilde{D}_{66}\frac{\partial^2 w}{\partial x\partial y}\frac{\partial^2 w}{\partial x\partial y}+4\tilde{D}_{66}^s\frac{\partial^2 w}{\partial x\partial y}\frac{\partial^2(\nabla^2 w)}{\partial x\partial y}$$
$$+2\tilde{H}_{66}^s\frac{\partial^2(\nabla^2 w)}{\partial x\partial y}\frac{\partial^2(\nabla^2 w)}{\partial x\partial y}+A_{55}^s\frac{\partial^3 w}{\partial y^3}\frac{\partial^3 w}{\partial y^3}+A_{44}^s\frac{\partial^3 w}{\partial x^3}\frac{\partial^3 w}{\partial x^3}]dxdy \tag{21}$$

$$K = 0.5\int_{-0.5a}^{0.5a}\int_{-0.5b}^{0.5b}[\tilde{I}_0(\frac{\partial w}{\partial t}\frac{\partial w}{\partial t}) + \mu\tilde{I}_0(\frac{\partial^2 w}{\partial x\partial t}\frac{\partial^2 w}{\partial x\partial t} + \frac{\partial^2 w}{\partial y\partial t}\frac{\partial^2 w}{\partial y\partial t}) + \tilde{I}_2(\frac{\partial^2 w}{\partial x\partial t}\frac{\partial^2 w}{\partial x\partial t} + \frac{\partial^2 w}{\partial y\partial t}\frac{\partial^2 w}{\partial y\partial t})$$
$$+\mu\tilde{I}_2(\frac{\partial^3 w}{\partial x^2\partial t}\frac{\partial^3 w}{\partial x^2\partial t} + 2\frac{\partial^3 w}{\partial x\partial y\partial t}\frac{\partial^3 w}{\partial x\partial y\partial t} + \frac{\partial^3 w}{\partial y^2\partial t}\frac{\partial^3 w}{\partial y^2\partial t}) + \tilde{K}_2(\frac{\partial^4 w}{\partial x^3\partial t}\frac{\partial^4 w}{\partial x^3\partial t} + \frac{\partial^4 w}{\partial y^3\partial t}\frac{\partial^4 w}{\partial y^3\partial t}) \quad (22)$$
$$+\mu\tilde{K}_2(\frac{\partial^5 w}{\partial x^4\partial t}\frac{\partial^5 w}{\partial x^4\partial t} + \frac{\partial^5 w}{\partial x^3\partial y\partial t}\frac{\partial^5 w}{\partial x^3\partial y\partial t} + \frac{\partial^5 w}{\partial x\partial y^3\partial t}\frac{\partial^5 w}{\partial x\partial y^3\partial t} + \frac{\partial^5 w}{\partial y^4\partial t}\frac{\partial^5 w}{\partial y^4\partial t})$$
$$+\tilde{J}_2(\frac{\partial^2 w}{\partial x\partial t}\frac{\partial^4 w}{\partial x^3\partial t} + \frac{\partial^2 w}{\partial y\partial t}\frac{\partial^4 w}{\partial y^3\partial t}) + \mu\tilde{J}_2(\frac{\partial^3 w}{\partial x^2\partial t}\frac{\partial^5 w}{\partial x^4\partial t} + \frac{\partial^3 w}{\partial x\partial y\partial t}\frac{\partial^5 w}{\partial x^3\partial y\partial t}$$
$$+\frac{\partial^3 w}{\partial x\partial y\partial t}\frac{\partial^5 w}{\partial x\partial y^3\partial t} + \frac{\partial^3 w}{\partial y^2\partial t}\frac{\partial^5 w}{\partial y^4\partial t})]dydx$$

in which

$$\begin{Bmatrix}\tilde{A}_{11},\tilde{D}_{11},\tilde{D}^s_{11},\tilde{H}^s_{11}\\ \tilde{A}_{12},\tilde{D}_{12},\tilde{D}^s_{12},\tilde{H}^s_{12}\\ \tilde{A}_{66},\tilde{D}_{66},\tilde{D}^s_{66},\tilde{H}^s_{66}\end{Bmatrix} = \int_{-h/2}^{h/2} Q_{11}(1,(z-z^*)^2,(z-z^*)(\Gamma-z^{**}),(\Gamma-z^{**})^2)\begin{Bmatrix}1\\ \upsilon\\ \frac{1-\upsilon}{2}\end{Bmatrix}dz \quad (23)$$

$$(\tilde{I}_0,\tilde{I}_2,\tilde{J}_2,\tilde{K}_2) = \int_{-h/2}^{h/2}(1,(z-z^*)^2,(z-z^*)(\Gamma-z^{**}),(\Gamma-z^{**})^2)\rho(z)dz \quad (24)$$

3. Solution approach

Based on Chebyshev-Ritz method, the dynamic buckling problem of a porous FG nanoplate will be solved in this section. First, the field components may be assumed in the following form

$$u(x,y,t) = R^u(x,y)\sum_{n=1}^{\infty}U_{nm}P_m(x)P_n(y)e^{i\omega_n t} \quad (25)$$

$$v(x,y,t) = R^v(x,y)\sum_{n=1}^{\infty}V_{mn}P_m(x)P_n(y)e^{i\omega_n t} \quad (26)$$

$$w(x,y,t) = R^w(x,y)\sum_{n=1}^{\infty}W_{mn}P_n(x)P_n(y)e^{i\omega_n t} \quad (27)$$

Consider the following essential boundary conditions:
Simply-supported (S):

$$w = \frac{\partial^2 w}{\partial x^2} = 0 \quad \text{at x=+0.5}a\text{, -0.5}a$$

$$w = \frac{\partial^2 w}{\partial y^2} = 0 \quad \text{at y=+ 0.5}b\text{, 0.5-}b$$

Clamped (C):

$w = \frac{\partial w}{\partial x} = 0$ at x=+0.5a, -0.5a and y=+0.5 b, -0.5b

Also, $P_m(x)$ is the n-th Chebyshev polynomials of the first kind may be expressed as

$$P_m(x) = \cos[(m-1)\arccos(\frac{2x}{a})]$$
$$P_n(y) = \cos[(n-1)\arccos(\frac{2y}{b})] \tag{28}$$

Also, R^i functions (i=u, v, w) are corresponding to the essential boundary conditions. Also, the genral form of R^i functions can be presented by

$$R^i(x,y) = (1+\frac{2x}{a})^{p^*}(1-\frac{2x}{a})^{q^*}(1+\frac{2y}{b})^{r^*}(1-\frac{2y}{b})^{s^*} \tag{29}$$

Note that p^* ,q^* , r*, s* rely on edge condition kind. In the case of CCCC condition, p^*= q^*=r*=s*=2 and for SSSS edges p^*= q^*=r*=s*=1. Substituting Eqs. (25)-(27) in $\Pi = (U+V-K) = 0$ and performing its minimization to unknown coefficients U_{mn}, V_{mn}, and W_{mn}, the below equation results in some algebraic equations in terms of unknowns.

$$\frac{\partial \Pi}{\partial U_{mn}} = \frac{\partial \Pi}{\partial V_{mn}} = \frac{\partial \Pi}{\partial W_{mn}} \tag{30}$$

The governing equations of periodically loaded FG plate in matrix form may be expressed as

$$[M]\{\ddot{W}_{mn}\} + [[K] + N_0(t)[G]]\{W_{mn}\} = 0 \tag{31}$$

in which [**M**] , [**K**] and [**G**] denote the mass, stiffness and geometrical stiffness matrices, respectively.

The periodic force with excitation frequency ϖ may be defined as $N_0(t) = -[\alpha + \beta\cos(\varpi t)]N_{cr}$, then the equations become

$$[M]\{\ddot{\Lambda}\} + [[K] - \{\alpha + \beta\cos(\varpi t)\}N_{cr}[G]]\{W_{mn}\} = 0 \tag{32}$$

Here, static and dynamic force components have been denoted by α and β and the excitation frequency is normalized as

$$\Omega = \varpi h\sqrt{\frac{\rho_c}{E_c}} \tag{33}$$

By assuming periodic coefficients of Mathieu–Hill kind, the solution becomes

$$[[K]-N_{cr}\{\alpha\pm 0.5\beta\}[G]-0.25\varpi[M]]\{W_{mn}\}=0 \tag{34}$$

Above equation must be solved numerically to derive instability regions. Further studies are based on following normalized coefficients

$$K_w=\frac{k_w a^4}{D_c}, K_p=\frac{k_p a^2}{D_c}, D_c=\frac{E_c h^3}{12(1-\nu_c^2)}, \mu=\frac{e_0 a}{a} \tag{35}$$

4. Results and discussions

This section contains obtained results for instability region of periodically loaded FG nanoplates having porosities. First, the instability regions of FG plates without porosities have been verified with those obtained by Han *et al*. (2015), as reported in Table 1. This table confirms that the proposed solution and plate formulation is correct. The results based on the proposed 3-unknown plate model are very close to the results of 4-unknown plate theory obtained by Han *et al.* (2015). But, the superiority of the proposed 3-unknwon model is that it provides simpler formulation and lower mathematical effort due to presenting fewer field components. Then, based on 3-variable plate theory and proposed solution, a convergence study has been presented in Table 2. Further investigations are based on 4 terms in the solution and the material properties are:

- E_c = 380 *GPa*, $\rho_c = 3800\ \ kg/m^3$, $\nu_c = 0.3$,
- E_m = 70 *GPa*, $\rho_m = 2707\ \ kg/m^3$, $\nu_m = 0.3$,

Fig. 2 illustrates the impact of static force component (α) and nonlocal constant (μ) on dynamical instability boundaries of porous FGM nanoplates when *a/h*=10, *p*=1 and K_w=K_p=0. The instability boundaries are clearly shown in first part of this figure. The right hand side of the instability boundaries is called instable region. One can find from the figure that as the static force component growths, the boundaries of dynamical stability will decrease at prescribed nonlocal coefficient. Also, it is clear that by increase of nonlocal coefficient, the dynamical stability boundary will be diminished. Moreover, the start point (β=0) will be decreased as nonlocal coefficient rises. This is because of plate stiffness reduction at nano-dimension interaction.

Table 1 Validation of normalized excitation frequency for FG plates at β=0.5

		α=0		α=0.1		α=0.2		α=0.3	
		Han *et al.* (2015)	present	Han *et al.* (2015)	present	Han *et al.* (2015)	present	Han *et al.* (2015)	present
$[\bar{K}]-(0.5\beta)N_{cr}[G]$	p=0.1	3.0113	3.01141	2.8033	2.80349	2.5787	2.57885	2.3325	2.33267
	p=1	2.9785	2.97861	2.7729	2.77295	2.5507	2.55075	2.3072	2.30725
	p=10	2.9365	2.93662	2.7337	2.73384	2.5147	2.51477	2.2746	2.2747
$[\bar{K}]+(0.5\beta)N_{cr}[G]$	p=0.1	3.8874	3.88761	3.7287	3.72889	3.5629	3.56309	3.389	3.3892
	p=1	3.8452	3.84531	3.6882	3.68830	3.5242	3.52431	3.3522	3.3523
	p=10	3.7910	3.79113	3.6362	3.63633	3.4745	3.47464	3.3049	3.30504

Table 2 A study of frequency convergence for proposed Chebyshev-Ritz approach (a/h=20).

m	μ =0	μ =1	μ =2
1	10.8639	10.3581	9.917
2	10.9427	10.4333	9.98902
3	9.86239	9.40898	9.01286
4	9.86239	9.40899	9.01286
5	9.86239	9.40899	9.01286
6	9.86239	9.40899	9.01286

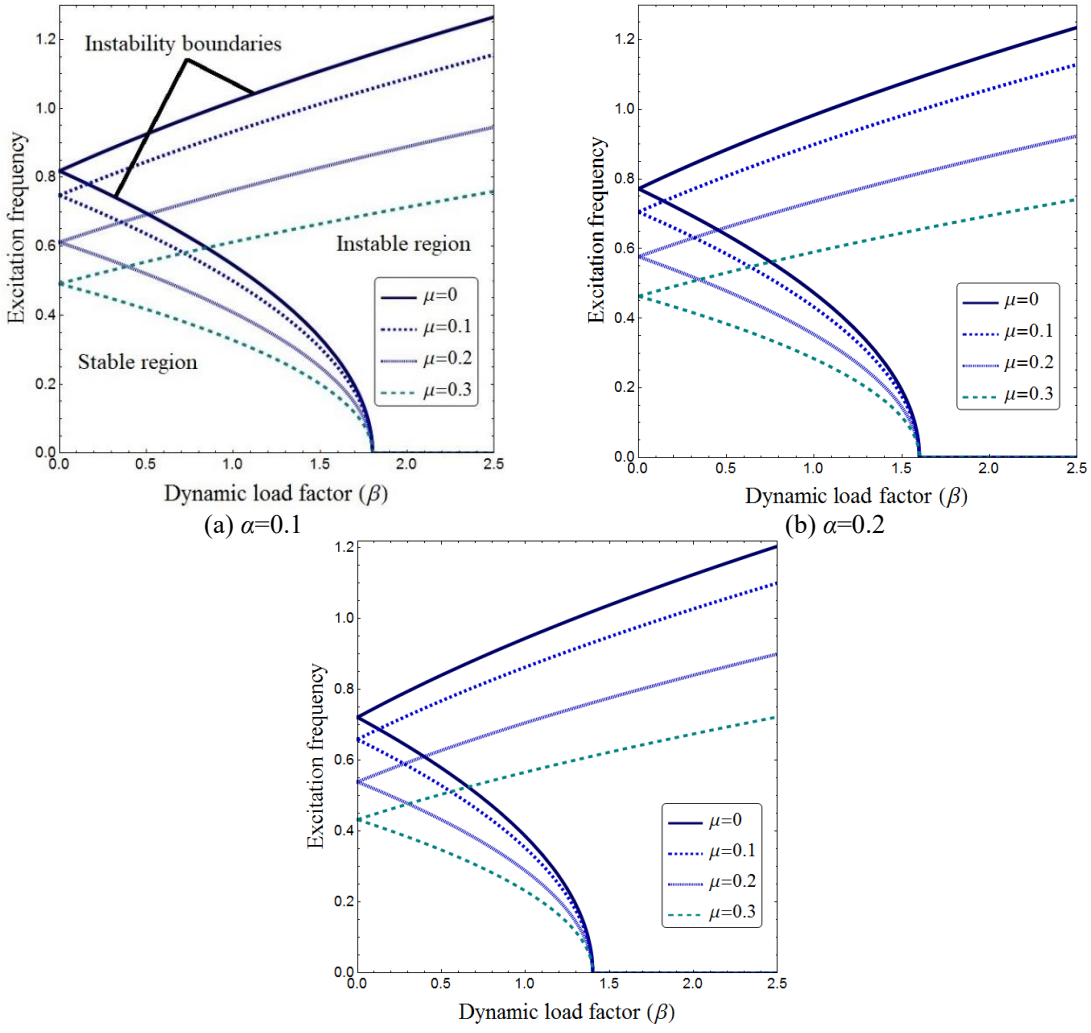

(a) α=0.1 (b) α=0.2

(c) α=0.3

Fig. 2 Normalized frequency according to dynamic force component based on various nonlocal and static force constants (p=1, p=1, ξ=0, K_w=0 ,K_p=0)

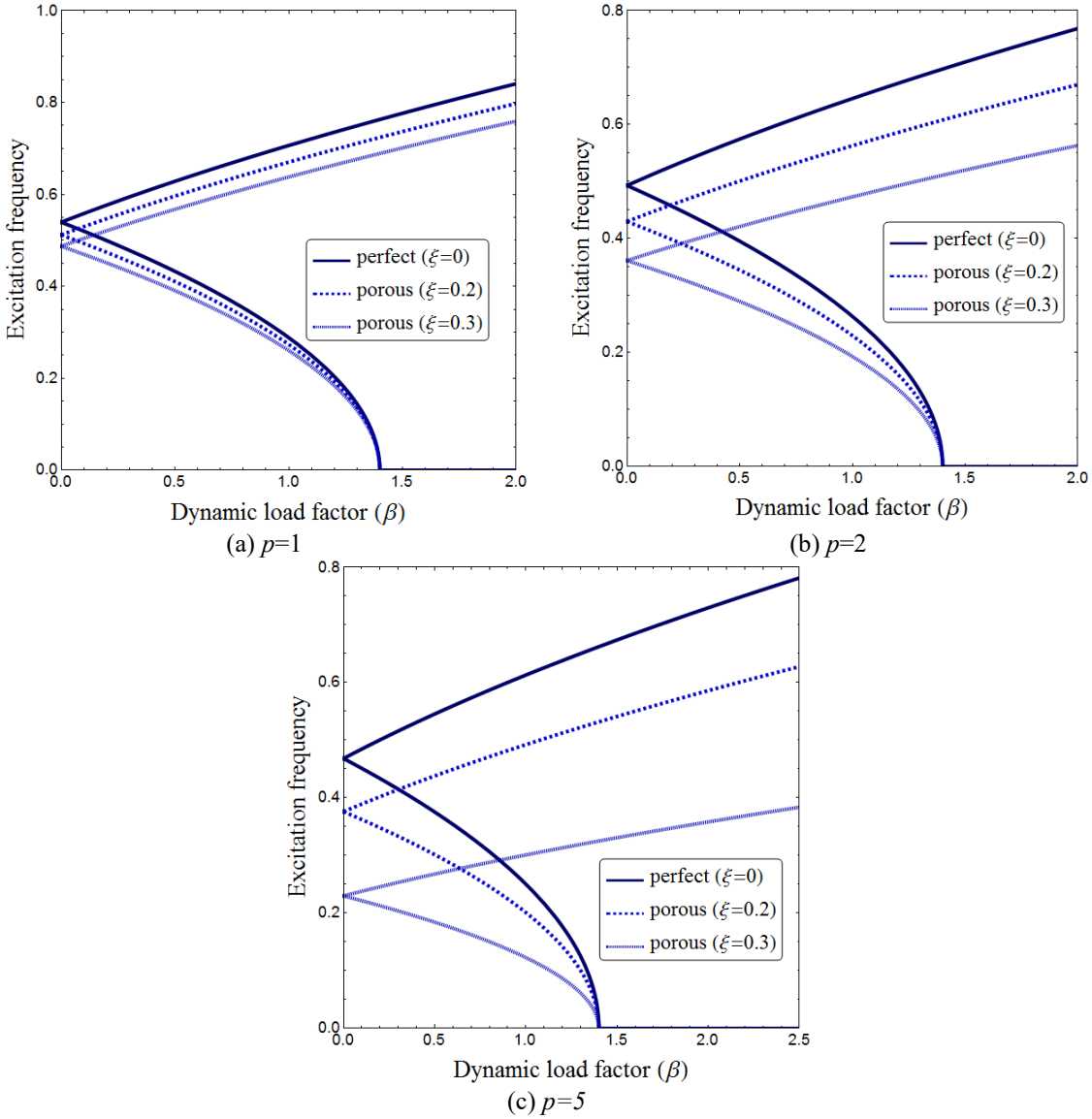

Fig. 3 Normalized frequency according to dynamic force component based on various material index and porosity amount (a/h=10, α=*0.3*, K_w=0, K_p=0)

Porosities amount influence on instability boundary of FGM nanoplate according to dynamical force component has been plotted in Fig. 3 when μ=0.2, *α=0.3* based of various material exponents. Increasing in porosities amount yields smaller vibration frequency due to decreasing the stiffness of nano-dimension plates. Moreover, the instability boundary gets smaller by the increasing of porosities amount. Thus, a porous FGM plates exposed periodic forces becomes more stable than non-porous plates. One can also find that by the decreasing of material exponent the instability region will increase. Actually, by the increment in material exponent value, the vibration natural frequency has been reduced.

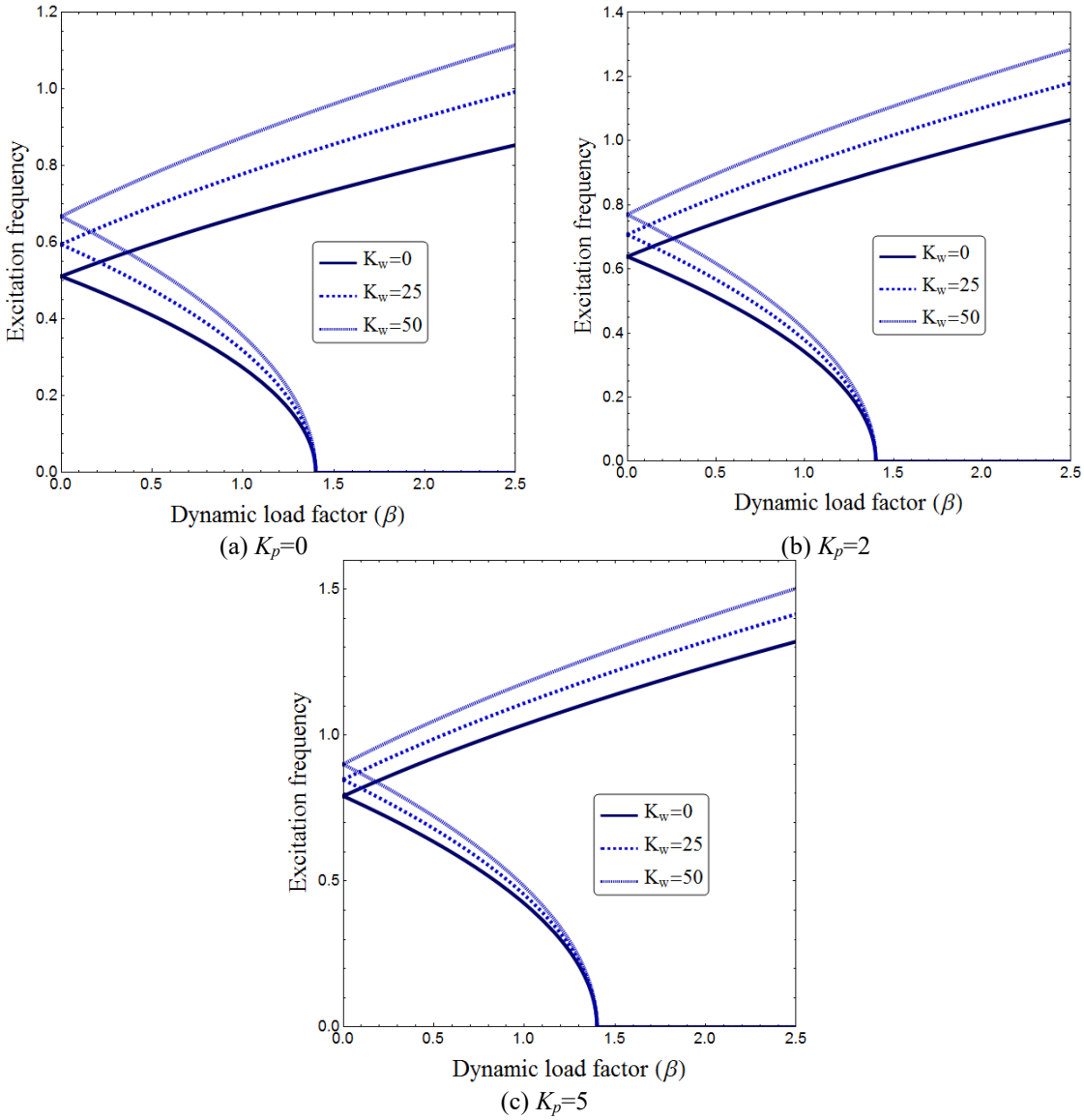

(a) K_p=0 (b) K_p=2

(c) K_p=5

Fig. 4 Normalized frequency according to dynamic force component based on various foundation constant (a/h=10, α=0.3, p=1, μ=0.2)

In Fig. 4, the changing of normalized excitation frequency according to dynamical force component (β) based on various elastic foundation constants is studied for simply-supported nanoplates when p =1, α=0.3 and μ=0.2. It is observable that increasing the foundation constants induces greater normalized excitation frequencies. Actually, by increasing in foundation constants, i.e. increasing in nanoplate bending stiffness, the dynamic buckling boundaries will be moved to upper regions of the origin.

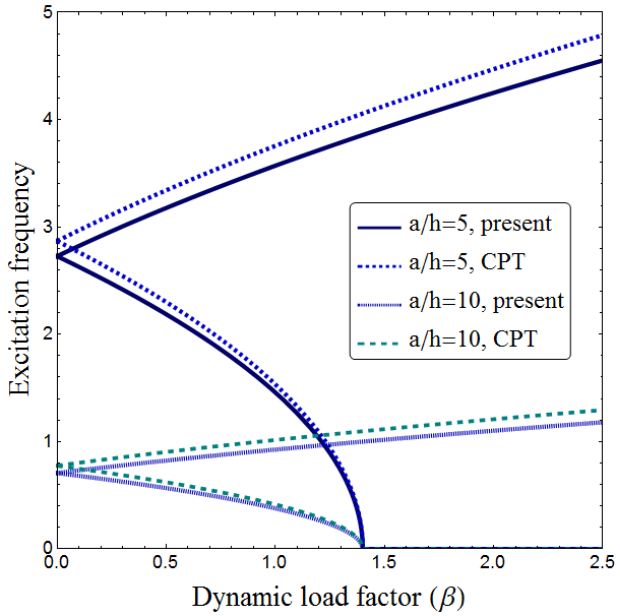

Fig. 5 Normalized frequency according to dynamic force component based on various plate models (p=1, α=0.3, μ=0.2, K_w=25, K_p=2)

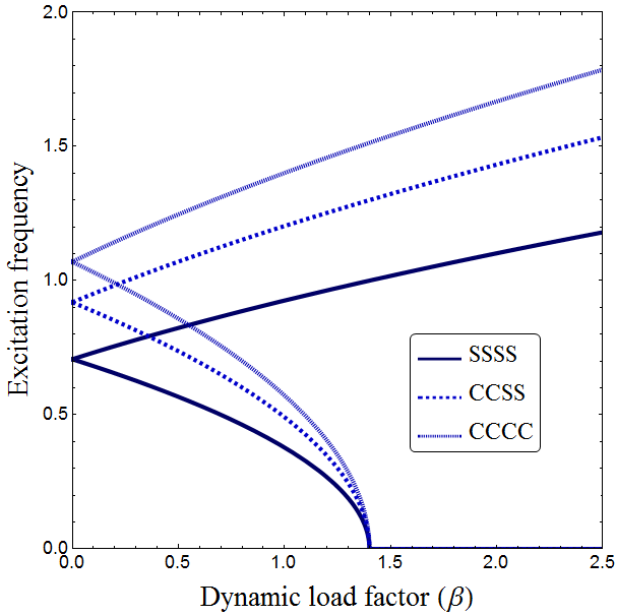

Fig. 6 Normalized frequency according to dynamic force component based on various boundary condition (p=1, a/h=10, α=0.3, μ=0.2, K_w=25, K_p=2)

Fig. 5 shows the normalized frequency of the nanoplate versus dynamical force component according to the classical and 3-unkonwn plate theories when $\alpha=0.3$, $p=1$, $\mu=0.2$, $K_w=25$, $K_p=2$. At affixed dynamic load factor, it can be seen that frequency results according to the classical plate theory are overestimated. In fact, more accurate examination of stability boundaries of FG nanoplates can be carried out employing higher order shear deformation plate theories. However, the value of side-to-thickness ratio has a remarkable influence on the instability boundaries. One can see that the width of instability boundaries for $a/h=10$ is smaller than that of $a/h=5$. In other words, excitation frequency reduces with the increasing of side-to-thickness ratio at a constant dynamical force component.

Also, Fig. 6 compares the effects of various boundary conditions on instability boundaries of FG nanoplates. One can confirm that at prescribed dynamical force component, the nanoplate having stronger boundary conditions provides greater excitation frequencies. Thus, CCCC boundary conditions provides greatest excitation frequencies.

5. Conclusions

This paper presented new results for instability regions of periodically loaded FG nanoplates having porosities based on a 3-variable plate theory. The solution was based on Chebyshev-Ritz-Bolotin method. It was seen that as the static force component raised, the boundaries of dynamical stability will decrease at prescribed nonlocal coefficient. Also, it was understood that by increase of nonlocal coefficient, the dynamical stability boundary diminished. Increasing in porosities amount led to smaller vibration frequency due to decreasing the stiffness of nano-dimension plates. Moreover, the instability boundary gets smaller by increasing of porosities amount. It was seen that increasing the foundation constants induced greater normalized excitation frequencies. Also, at prescribed dynamical force component, the nanoplate having stronger boundary conditions provided greater excitation frequencies.

Acknowledgments

The authors would like to thank Mustansiriyah university (www.uomustansiriyah.edu.iq) Baghdad-Iraq for its support in the present work.

References

Ahmed, R.A., Fenjan, R.M. and Faleh, N.M. (2019), "Analyzing post-buckling behavior of continuously graded FG nanobeams with geometrical imperfections", *Geomech. Eng.*, **17**(2), 175-180.

Atmane, H.A., Tounsi, A. and Bernard, F. (2015a), "Effect of thickness stretching and porosity on mechanical response of a functionally graded beams resting on elastic foundations", *Int. J. Mech. Mater. Des.*, 1-14.

Atmane, H.A., Tounsi, A., Bernard, F. and Mahmoud, S.R. (2015b), "A computational shear displacement model for vibrational analysis of functionally graded beams with porosities", *Steel Compos. Struct.*, **19**(2), 369-384.

Bakhadda, B., Bouiadjra, M.B., Bourada, F., Bousahla, A.A., Tounsi, A. and Mahmoud, S.R., (2018), "Dynamic and bending analysis of carbon nanotube-reinforced composite plates with elastic foundation", *Wind Struct.*, **27**(5), 311-324.

Belabed, Z., Bousahla, A.A., Houari, M.S.A., Tounsi, A. and Mahmoud, S.R. (2018), "A new 3-unknown hyperbolic shear deformation theory for vibration of functionally graded sandwich plate", *Earthq. Struct.*, **14**(2), 103-115.

Bellifa *et al*. (2017), "A nonlocal zeroth-order shear deformation theory for nonlinear postbuckling of nanobeams", *Struct. Eng. Mech.*, **62**(6), 695 - 702.

Belkorissat, I., Houari, M.S.A., Tounsi, A., Bedia, E.A. and Mahmoud, S.R. (2015), "On vibration properties of functionally graded nano-plate using a new nonlocal refined four variable model", *Steel Compos. Struct.*, **18**(4), 1063-1081.

Bouafia *et al*. (2017), "A nonlocal quasi-3D theory for bending and free flexural vibration behaviors of functionally graded nanobeams", *Smart Struct. Syst*., **19**(2), 115-126.

Bouadi *et al*. (2018), "A new nonlocal HSDT for analysis of stability of single layer graphene sheet", *Adv. Nano Res.*, **6**(2), 147-162.

Cherif et al. (2018), "Vibration analysis of nano beam using differential transform method including thermal effect", *J. Nano Res.*, **54**, 1-14.

Eringen, A.C. (1983), "On differential equations of nonlocal elasticity and solutions of screw dislocation and surface waves", *J. Appl. Phys.*, **54**(9), 4703-4710.

Faleh, N.M., Ahmed, R.A. and Fenjan, R.M. (2018). "On vibrations of porous FG nanoshells. *International J. Eng. Sci.*, **133**, 1-14.

Hachemi, H., *et al.* (2017), "A new simple three-unknown shear deformation theory for bending analysis of FG plates resting on elastic foundations", *Steel Compos. Struct.*, **25**(6), 717-726.

Han, S.C., Park, W. and Jung, W.Y. (2015), "A four-variable refined plate theory for dynamic stability analysis of S-FGM plates based on physical neutral surface", *Compos. Struct.*, **131**, 1081-1089.

Hosseini, M. and Jamalpoor, A. (2015), "Analytical solution for thermomechanical vibration of double-viscoelastic nanoplate-systems made of functionally graded materials", *J. Therm. Stresses*, **38**(12), 1428-1456.

Houari, M.S.A., Tounsi, A., Bessaim, A. and Mahmoud, S.R. (2016). "A new simple three-unknown sinusoidal shear deformation theory for functionally graded plates", *Steel Compos Struc.t*, **22**(2), 257-276.

Kaci et al. (2018), "Post-buckling analysis of shear-deformable composite beams using a novel simple two-unknown beam theory", *Structural Engineering and M*echanics, **65**(5), 621-631.

Karami, B., Janghorban, M. and Tounsi, A. (2018a), "Nonlocal strain gradient 3D elasticity theory for anisotropic spherical nanoparticles", *Steel Compos. Struct.*, **27**(2), 201-216. http://dx.doi.org/10.12989/scs.2018.27.2.201

Karami, B., Shahsavari, D., Nazemosadat, S.M.R., Li, L. and Ebrahimi, A. (2018b), "Thermal buckling of smart porous functionally graded nanobeam rested on Kerr foundation", *Steel Compos. Struct.*, **29**(3), 349-362. http://dx.doi.org/10.12989/scs.2018.29.3.349.

Khetir et al. (2017), "A new nonlocal trigonometric shear deformation theory for thermal buckling analysis of embedded nanosize FG plates", *Struct. Eng. Mech*., **64**(4), 391-402.

Larbi Chaht et al. (2015), "Bending and buckling analyses of functionally graded material (FGM) size-dependent nanoscale beams including the thickness stretching effect", *Steel Compos. Struct*., **18**(2), 425-442.

Mahmoudi, A., Benyoucef, S., Tounsi, A., Benachour, A. and Bedia, E. A. A. (2018). "On the effect of the micromechanical models on the free vibration of rectangular FGM plate resting on elastic foundation", *Earthq. Struct.*, **14**(2), 117-128.

Malikan, M., Tornabene, F. and Dimitri, R. (2018b), "Nonlocal three-dimensional theory of elasticity for buckling behavior of functionally graded porous nanoplates using volume integrals", Mater. Res. Express, 5(9), 095006.

Mechab, B., Mechab, I., Benaissa, S., Ameri, M. and Serier, B. (2016). "Probabilistic analysis of effect of the porosities in functionally graded material nanoplate resting on Winkler–Pasternak elastic foundations", *Appl. Math. Model.*, **40**(2), 738-749.

Mehala, T., Belabed, Z., Tounsi, A. and Beg, O.A. (2018), "Investigation of influence of homogenization models on stability and dynamics of FGM plates on elastic foundations", *Geomech. Eng*., **16**(3), 257-271.

Mokhtar, Y., *et al.* (2018), "A novel shear deformation theory for buckling analysis of single layer graphene sheet based on nonlocal elasticity theory", *Smart Struct. Syst.*, **21**(4), 397-405.
Mouffoki, A., *et al*. (2017), "Vibration analysis of nonlocal advanced nanobeams in hygro-thermal environment using a new two-unknown trigonometric shear deformation beam theory", *Smart Struct. Syst*., **20**(3), 369-383.
Natarajan, S., Chakraborty, S., Thangavel, M., Bordas, S. and Rabczuk, T. (2012). "Size-dependent free flexural vibration behavior of functionally graded nanoplates", *Comput. Mater. Sci.*, **65**, 74-80.
Reddy, J.N. (1990), "A general non-linear third-order theory of plates with moderate thickness", *Int. J. Non-linear Mech.*, **25**(6), 677-686.
Sadoun, M., Houari, M.S.A., Bakora, A., Tounsi, A., Mahmoud, S.R. and Alwabli, A.S. (2018), "Vibration analysis of thick orthotropic plates using quasi 3D sinusoidal shear deformation theory", *Geomech. Eng.*, **16**(2), 141-150.
Shahverdi, H. and Barati, M.R. (2017), "Vibration analysis of porous functionally graded nanoplates", Int. J. Eng. Sci., 120, 82-99. https://doi.org/10.1016/j.ijengsci.2017.06.008.
She, G.L., Yuan, F.G., Ren, Y.R. and Xiao, W.S. (2017), "On buckling and postbuckling behavior of nanotubes", Int. J. Eng. Sci., 121, 130-142. https://doi.org/10.1016/j.ijengsci.2017.09.005.
She, G.L., Yan, K.M., Zhang, Y.L., Liu, H.B. and Ren, Y.R. (2018a), "Wave propagation of functionally graded porous nanobeams based on non-local strain gradient theory", *Euro. Phys. J. Plus*, **133**(9), 368. https://doi.org/10.1140/epjp/i2018-12196-5.
She, G.L., Ren, Y.R., Yuan, F.G. and Xiao, W.S. (2018b), "On vibrations of porous nanotubes", *Int. J. Eng. Sci*., **125**, 23-35. https://doi.org/10.1016/j.ijengsci.2017.12.009
She, G.L., Ren, Y.R. and Yan, K.M. (2019a), "On snap-buckling of porous FG curved nanobeams", *Acta Astronautica*, **161**, 475-484. https://doi.org/10.1016/j.actaastro.2019.04.010
She, G.L, Jiang, XY. and Karami, B. (2019b), "On thermal snap-buckling of FG curved nanobeams", Mater. Res. Express, 6, 115008. https://doi.org/10.1088/2053-1591/ab44f1
Shafiei, N. and She, G.L. (2018), "On vibration of functionally graded nano-tubes in the thermal environment", *Int. J. Eng. Sci.*, **133**, 84-98.
Taj, M.G., Chakrabarti, A. and Sheikh, A.H. (2013), "Analysis of functionally graded plates using higher order shear deformation theory. *Applied Mathematical Mo*delling, **37**(18), 8484-8494.
Thai, H.T., Vo, T., Bui, T. and Nguyen, T.K. (2014), "A quasi-3D hyperbolic shear deformation theory for functionally graded plates", *Acta Mechanica*, **225**(3), 951-964.
Yahia, S.A., *et al*. (2015), "Wave propagation in functionally graded plates with porosities using various higher-order shear deformation plate theories", *Struct. Eng. Mech*., **53**(6), 1143-1165.
Yazid, M., *et al.* (2018), "A novel nonlocal refined plate theory for stability response of orthotropic single-layer graphene sheet resting on elastic medium", *Smart Struct. Syst*., **21**(1), 15-25.
Zemri, A., *et al.* (2015), "A mechanical response of functionally graded nanoscale beam: an assessment of a refined nonlocal shear deformation theory beam theory", *Struct. Eng. Mech.*, **54**(4), 693-710.
Zenkour, A.M. (2009), "The refined sinusoidal theory for FGM plates on elastic foundations", *Int. J. Mech. Sci.*, **51**(11), 869-880.
Zenkour, A.M. (2016), "Nonlocal transient thermal analysis of a single-layered graphene sheet embedded in viscoelastic medium", *Physica E: Low-dimensional Syst. Nanostruct.*, **79**, 87-97.
Zenkour, A.M. (2018), "A quasi-3D refined theory for functionally graded single-layered and sandwich plates with porosities", *Compos. Struct*., **201**, 38-48. https://doi.org/10.1016/j.compstruct.2018.05.147.
Zenkour, A.M. and Radwan, A.F. (2019), "Bending response of FG plates resting on elastic foundations in hygrothermal environment with porosities", *Compos. Struct*., **213**, 133-143. https://doi.org/10.1016/j.compstruct.2019.01.065.
Zidi, M., *et al*. (2017), "A novel simple two-unknown hyperbolic shear deformation theory for functionally graded beams", *Struct. Eng. Mech*., **64**(2), 145-153.